Electronic Supplementary Material (ESI) for Dalton Transactions.

A 2D/2D NiCo-MOF/Ti_3C_2 heterostructure for simultaneous detection of acetaminophen, dopamine and uric acid by differential pulse voltammetry

Xing Lu[a], Feng Zhang[*a,b], Yimeng Sun[a], Kai Yu[a], Wei Guo[a] and Fengyu Qu[*a,b]

a. Key Laboratory of Photochemical Biomaterials and Energy Storage Materials, Heilongjiang Province, Harbin Normal University, Harbin 150025, P. R. China

b. Key Laboratory of Photonic and Electronic Bandgap Materials, Ministry of Education, Harbin Normal University, Harbin 150025, P. R. China

**Corresponding authors: Feng Zhang (E-mail: zhangfeng@hrbnu.edu.cn) and Fengyu Qu (E-mail: qufengyu@hrbnu.edu.cn)*

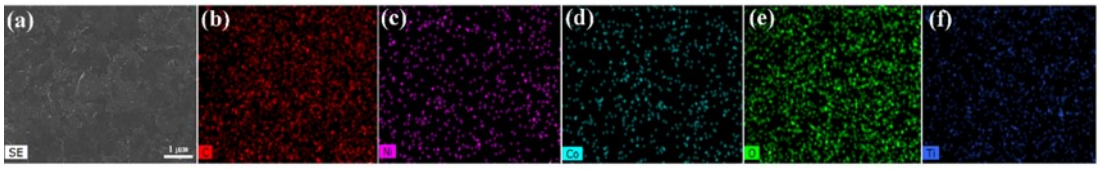

Fig. S1 SEM image and the corresponding elemental mapping images of NiCo-MOF/Ti_3C_2.

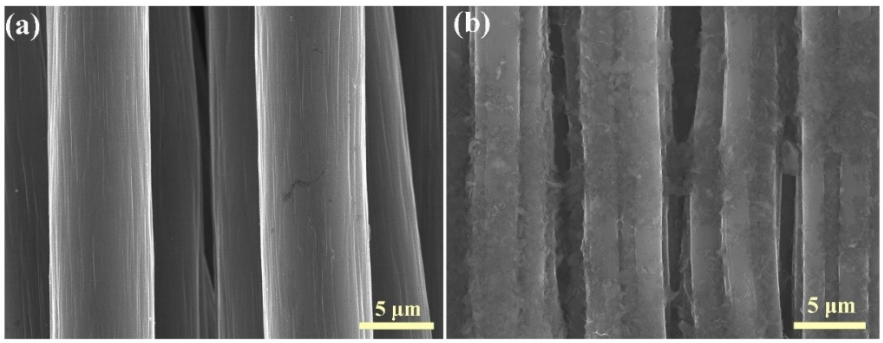

Fig. S2 SEM images of (a) CCE and (b) NiCo-MOF/Ti_3C_2/CCE.

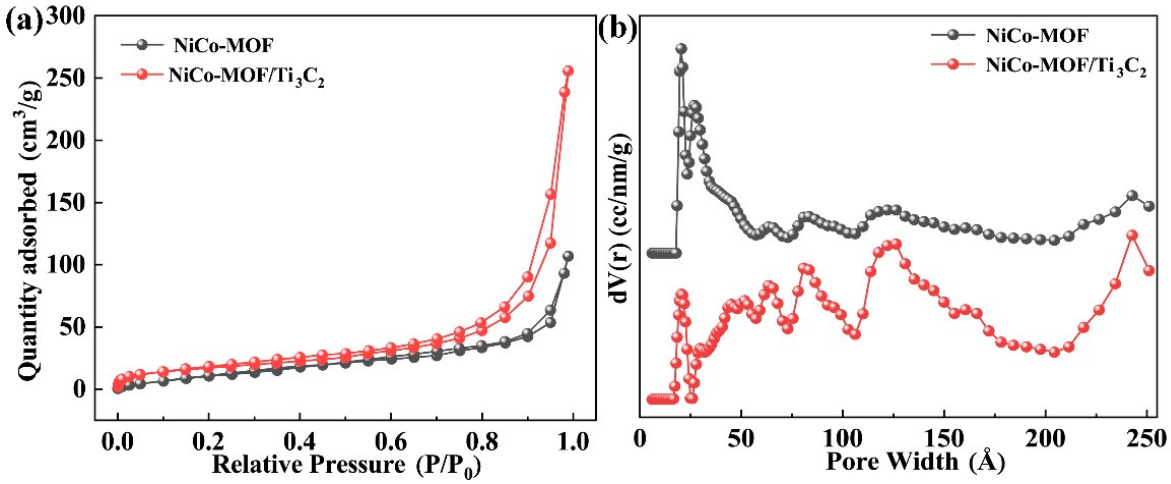

Fig. S3 (a) The N_2 adsorption-desorption curves and (b) the corresponding pore size distribution of NiCo-MOF and NiCo-MOF/Ti_3C_2.

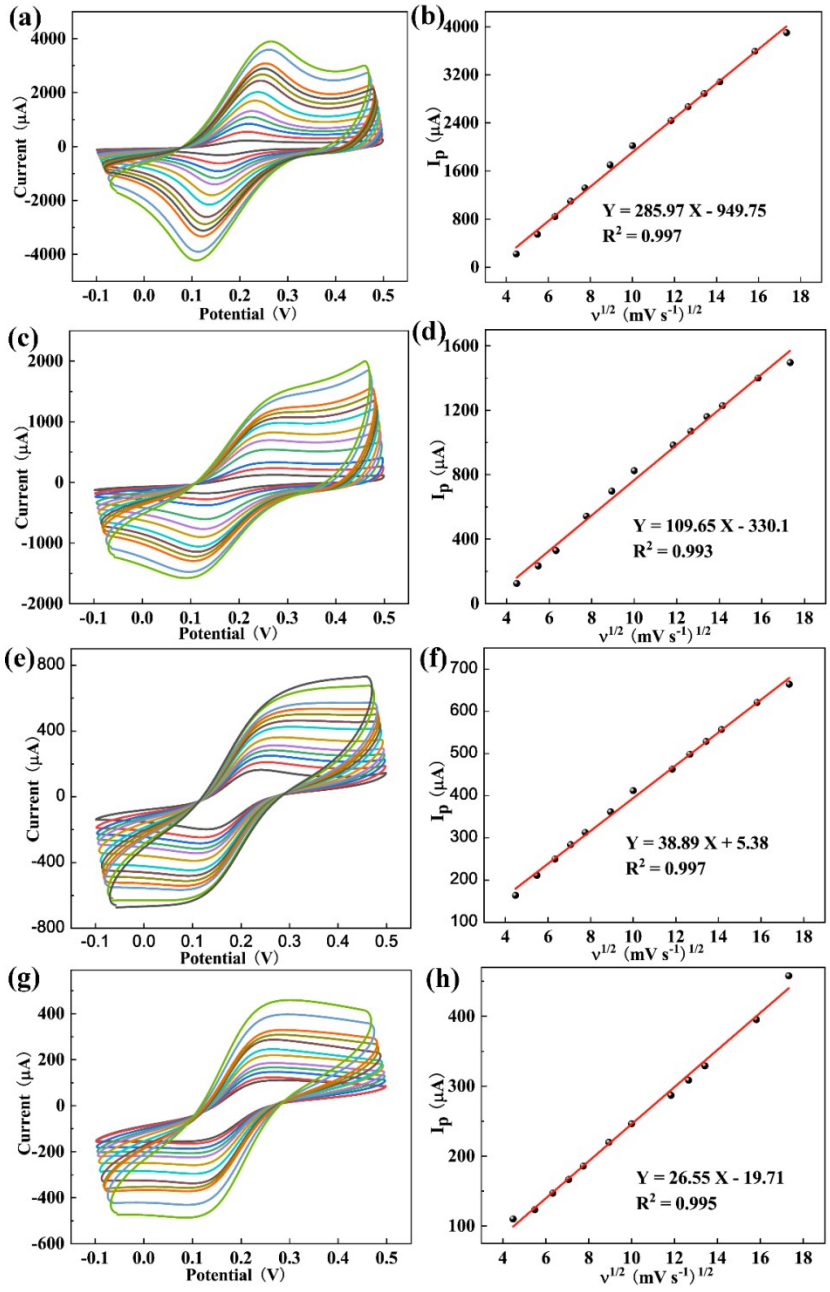

Fig. S4 CV curves of (a) NiCo-MOF/Ti_3C_2/CCE, (c) Ti_3C_2/CCE, (e) NiCo-MOF/CCE and (g) CCE recorded in 0.1 M KCl containing 1 mM $K_3[Fe(CN)_6]$ at scan rates varied from 0.02 to 0.30 V s^{-1}; (b, d, f and h) the dependence plots of peak current vs. square root of scan rate ($\upsilon^{1/2}$).

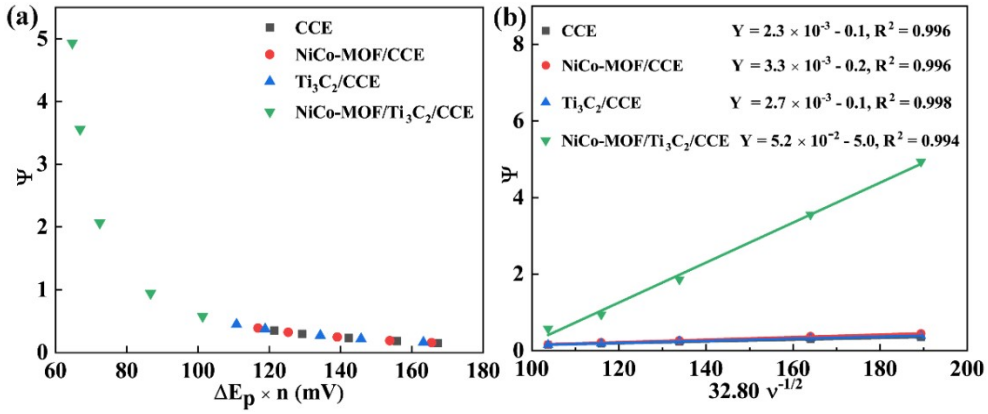

Fig. S5 (a) Plot of ψ vs. $\Delta E_p \times n$ for different electrodes under disparate scan rates (30, 40, 60, 80, 100 mV/s); (b) the relationships of ψ vs. 32.80 $v^{-1/2}$

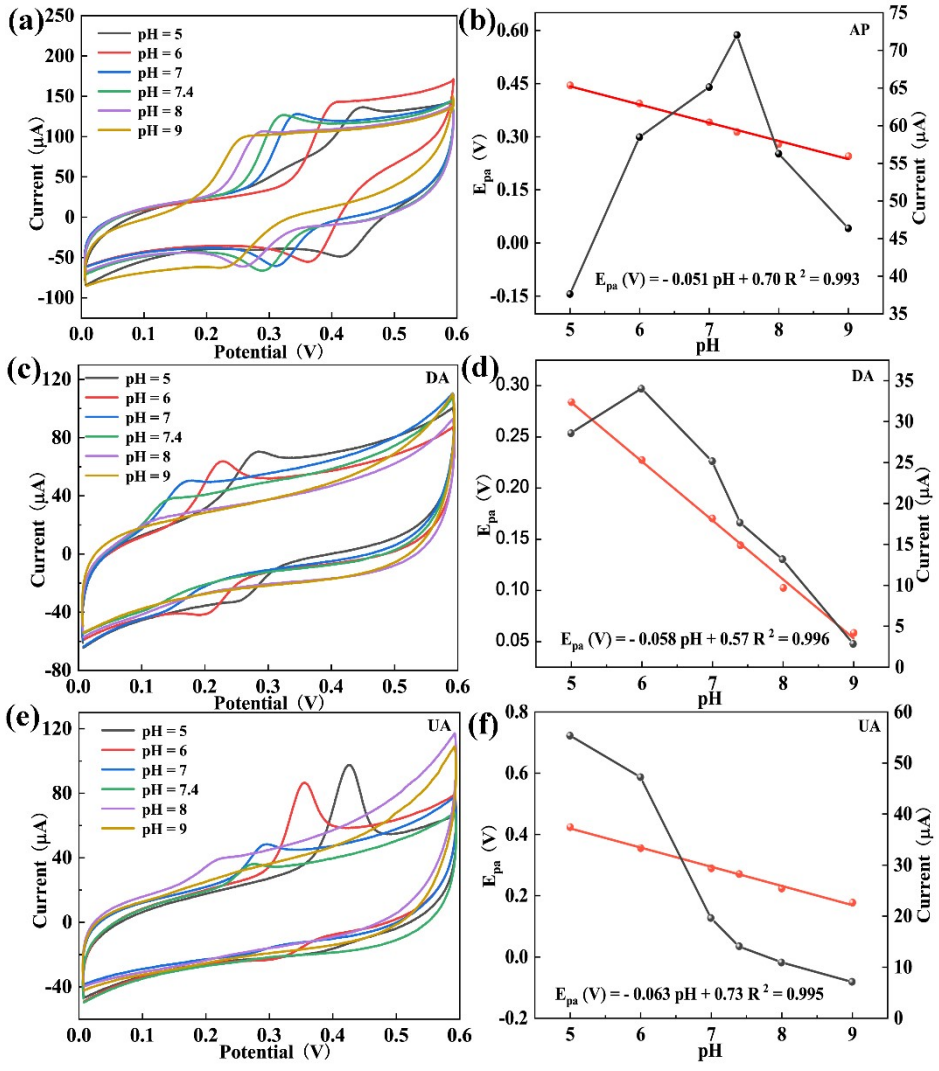

Fig. S6 (a, c and e) CVs on NiCo-MOF/Ti_3C_2/CCE in 0.1 M PB with different pH values (5.0 to 9.0) containing 20 μM AP, DA and UA; (b, d and f) the plots of peak current vs. pH value, and the peak potential vs. pH value.

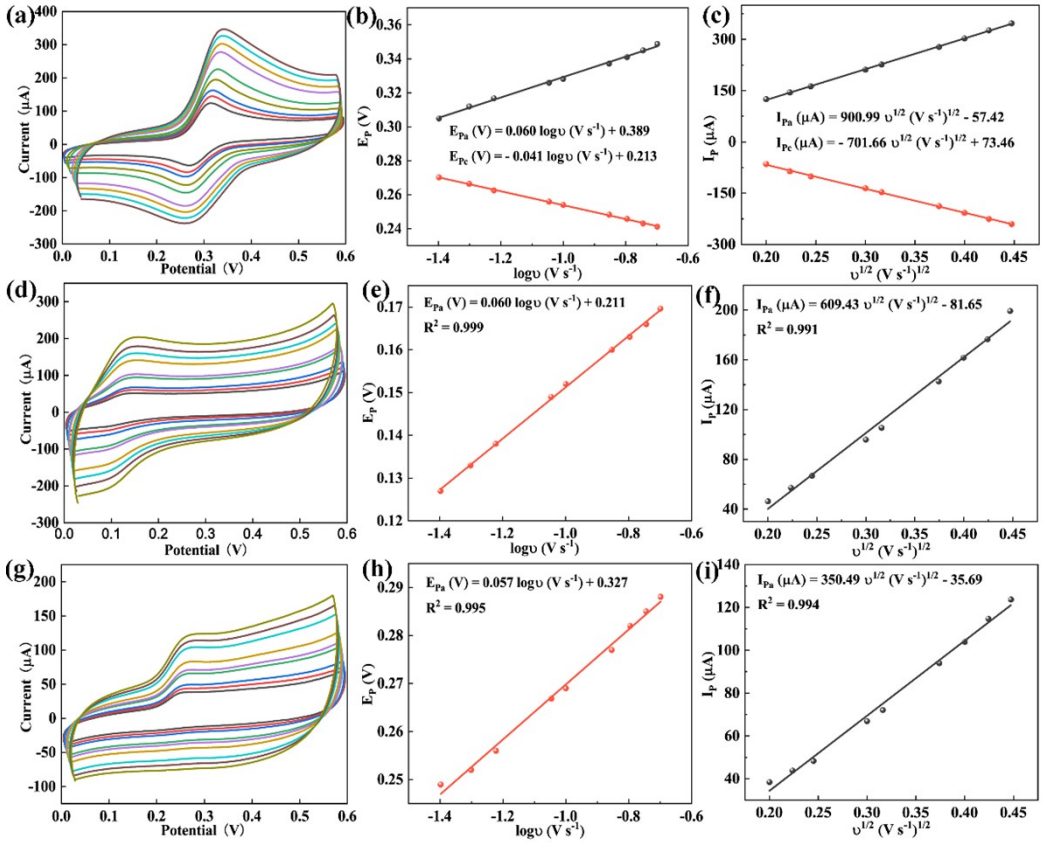

Fig. S7 (a, d and g) CV curves of NiCo-MOF/Ti_3C_2/CCE in 0.1 M PB (pH 7.4) containing 30 μM AP, DA and UA recorded at different scan rates (40 to 200 mV s^{-1}); (b, e and h) the linearity plots of I_p vs. ($υ^{1/2}$) and (c, f and i) E_p *vs.* log υ.

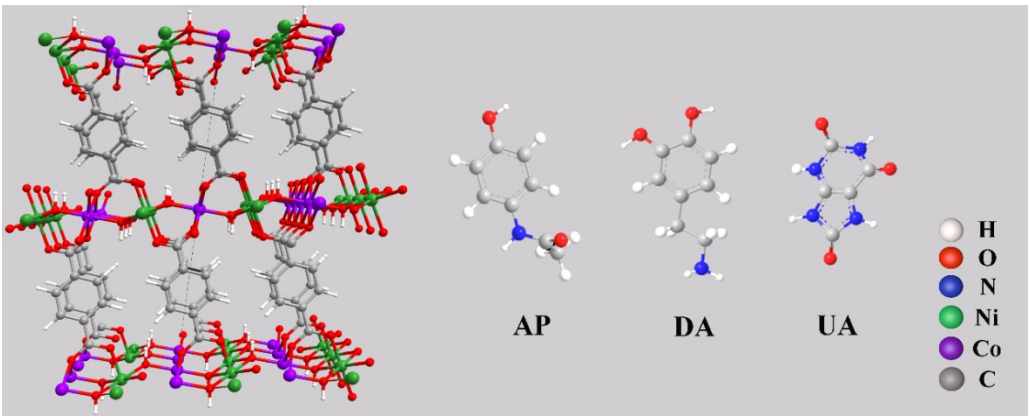

Fig. S8 Crystal structure of NiCo-MOF and structure of AP, DA and UA.

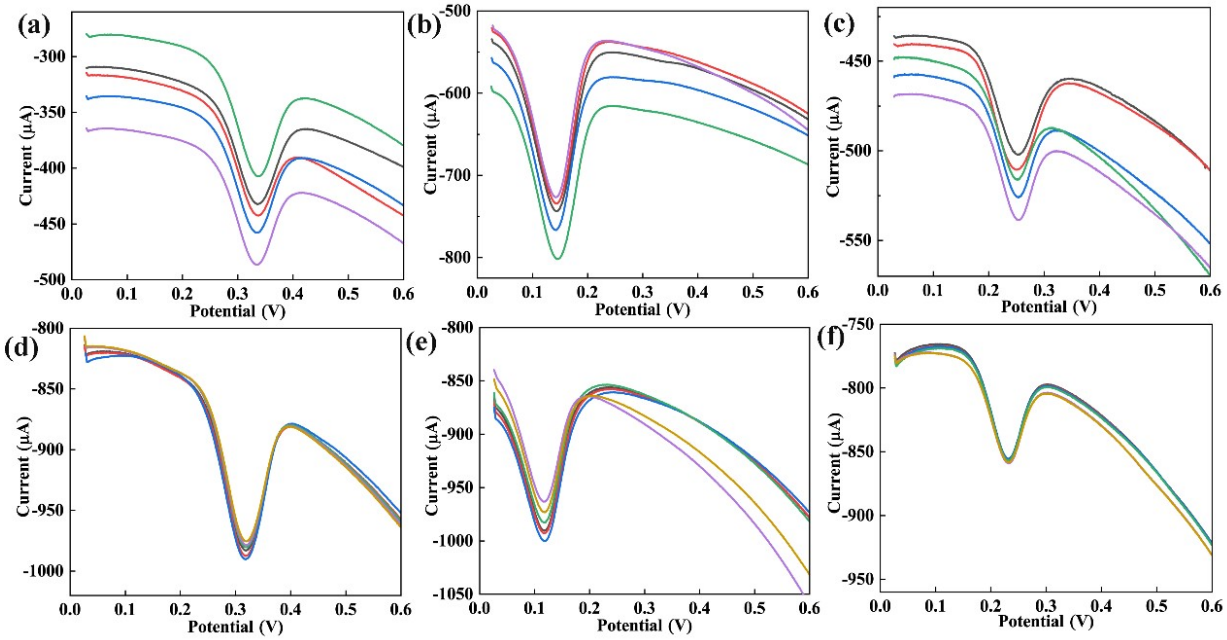

Fig. S9 The DPV curves of five successive measurements with the same electrode and six different measurements with disparate batches of electrodes.

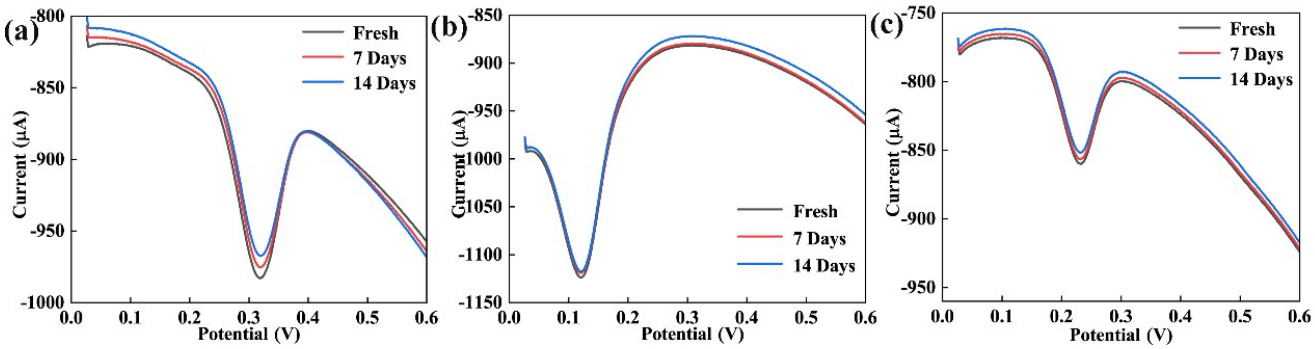

Fig. S10 The DPV curves of NiCo-MOF/Ti_3C_2/CCE toward (a) AP (200 μM), (b) DA (100 μM) and (c) UA (100 μM) within 14 days.

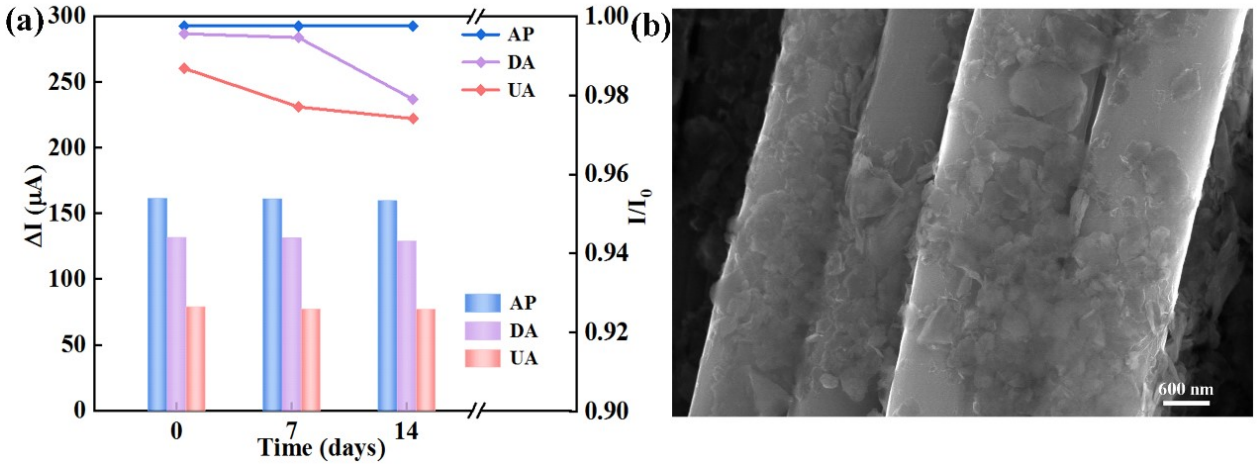

Fig. S11 (a) The current response of NiCo-MOF/Ti_3C_2/CCE toward 20 μM AP, DA UA within 14 days; (b) SEM image of NiCo-MOF/Ti_3C_2/CCE after electrochemical test.

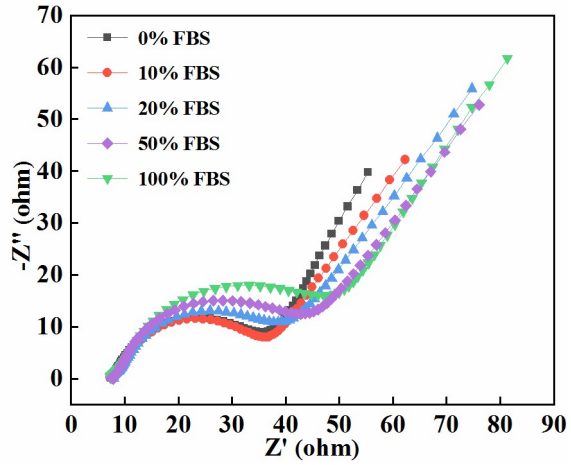

Fig. S12 (a) EIS of NiCo-MOF/Ti_3C_2/CCE after immersing in FBS solution under different dilution ratios.

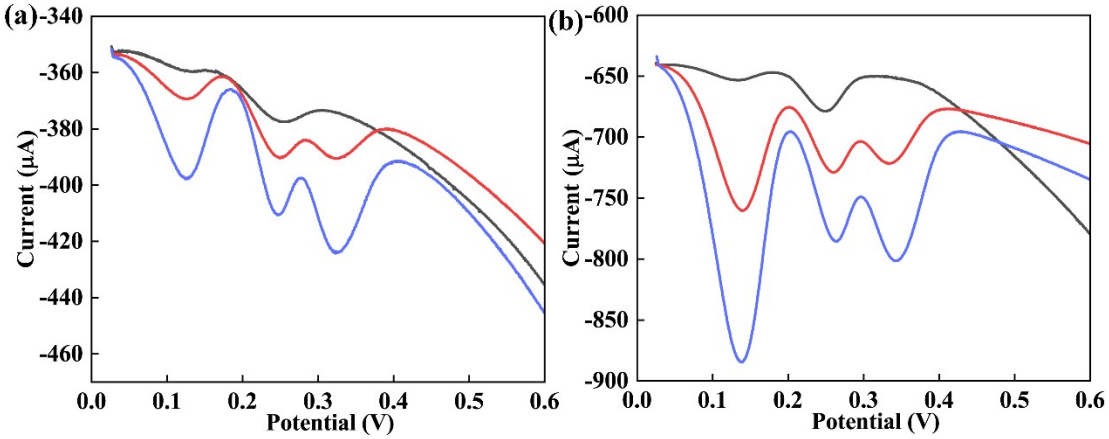

Fig.S13 (a) DPV curves in diluted serum containing standard solution DA(0, 7, 30 μM), UA(0, 18, 50 μM) and AP (0, 4,70 μM); (b) DPV curves in diluted urine containing standard solution DA(0, 90, 200 μM), UA (0, 80, 180 μM) and AP (0, 85, 250 μM).

The procedures of actual samples detection are as follows:

(i) The serum was purchased from KEJING Biology Co. Ltd, and got urine from normal people. Before the experiment, the serum and urine were centrifuged to obtain the supernatant, and then diluted

100 times (by volume) with 0.1 M PB (pH 7.4).

(ii) Pipette 10 mL of the diluted samples into vial to proceed DPV analysis by a three-electrode system, and then the amounts of DA and UA were determined according to the linear equation of analyte concentration vs. current response in PB.

(iii) The standard addition method is used next to assess the practicability of the fabricated biosensor. The known amount of DA, UA and AP were added into the diluted samples, and were measured their DPV curves. The current response was compared with the standard curve in PB to calculate the recovery.

Table S1 The reported methods towards AP, DA and UA detection compared to NiCo-MOF/Ti_3C_2/CCE.

Eletrodes	Techniques	Linear range(μM)			LOD (μM)			Ref.
		AP	DA	UA	AP	DA	UA	
$K_2Fe_4O_7$-GCE	DPV	−	1−140	−	−	0.22	−	[1]
Au NPs@3D GR/ITO	DPV	−	0.1−60	0.1−60	−	0.1	0.1	[2]
HKUST-1/GCE	DPV	12.5−275	12.5−175	−	0.092	0.11	−	[3]
Pt/CeO_2@Cu_2O−CPE	DPV	0.5−160	0.5−160	−	0.091	0.079	−	[4]
MoS_2–TiO_2/rGO/SPE	DPV	0.1–125	−	−	0.046	−	−	[5]
MIPs/pThi/NPG	DPV	−	0.3−100	−	0.1	−	−	[6]
CNCo/GCE	DPV	−	−	2–110	−	−	0.83	[7]
Cu/Cu_xO NPs/PGE	DPV	−	0.3−53	−	−	1.07	−	[8]
MIP/NPGL	DPV	−	2−180	5−160	−	0.3	0.4	[9]
NiCo-MOF/Ti_3C_2/CCE	DPV	0.01−400	0.01−300	0.01−350	0.008	0.004	0.006	This work

Table S2 The reproducibility of NiCo-MOF/Ti_3C_2/CCE.

	Analytes	I_1/μA	I_2/μA	I_3/μA	I_4/μA	I_5/μA	I_6/μA	RSD/%
The same	AP	118.77	121.07	124.14	119.46	120.92	-	1.50%
electrode	DA	204.65	208.87	204.27	203.04	204.19	-	0.97%
	UA	65.41	68.63	66.94	67.25	68.24	-	1.68%
Different	AP	161.79	165.24	162.17	164.70	163.17	161.33	0.90%
electrodes	DA	125.52	123.76	125.44	121.46	124.68	123.60	1.11%
	UA	77.21	74.61	77.29	73.99	75.30	72.15	2.40%

Reference

1 X. Sun, L. Zhang, X. Zhang, X. Liu, J. Jian, D. Kong, D. Zeng, H. Yuan and S. Feng, Electrochemical dopamine sensor based on superionic conducting potassium ferrite. *Biosens. Bioelectron.* 2020, **153**,112045.

2 Z. Wang, H. Y. Yue, S. Huang, Z. M. Yu, X. Gao, H. T. Chen, W. Q. Wang, S. S. Song, E. H. Guan and H. J. Zhang, Gold nanoparticles anchored onto three-dimensional graphene: simultaneous voltammetric determination of dopamine and uric acid. *Microchim. Acta*. 2019, **186**, 573.

3 F.A . Sofi, M. A. Bhat and K. Majid, Cu^{2+}-BTC based metal–organic framework: a redox accessible and redox stable MOF for selective and sensitive electrochemical sensing of acetaminophen and dopamine. *New J. Chem.* 2019, **43**, 3119-3127.

4 A. R. Rajamani and S. C. Peter, Novel Nanostructured Pt/CeO_2@Cu_2O Carbon-Based Electrode To Magnify the Electrochemical Detection of the Neurotransmitter Dopamine and Analgesic Paracetamol. *ACS Applied Nano Materials*. 2018, **1**, 5148-5157.

5 N. Demir, K. Atacan, M. Ozmen and S. Z. Bas, Design of a new electrochemical sensing system based on MoS_2–TiO_2/reduced graphene oxide nanocomposite for the detection of paracetamol. *New J. Chem.* 2020, **44**, 11759-11767.

6 J. Yang, Y. Hu and Y. Li, Molecularly imprinted polymer-decorated signal on-off ratiometric electrochemical sensor for selective and robust dopamine detection. *Biosens. Bioelectron.* 2019, **135**, 224-230.

7 L. Liu, L. Liu, Y. Wang and B. C. Ye, A novel electrochemical sensor based on bimetallic metal-organic framework-derived porous carbon for detection of uric acid. *Talanta*. 2019, **199**, 478-484.

8 E. Bahrami, R. Amini and S. Vardak, Electrochemical detection of dopamine via pencil graphite electrodes modified by Cu/Cu_xO nanoparticles. *J. Alloys Compd.* 2021, **855**, 157292.

9 N. Li, C. Nan, X. Mei, Y. Sun, H. Feng and Y. Li, Electrochemical sensor based on dual-template molecularly imprinted polymer and nanoporous gold leaf modified electrode for simultaneous determination of dopamine and uric acid. *Microchim. Acta*. 2020, **187**, 496.